

## **MODIS QUARTERLY REPORT: JAN/01/98 - MAR/31/98**

### **Radiative Transfer Based Synergistic MODIS/MISR Algorithm for the Estimation of Global LAI & FPAR**

J. Knjazihhin, Y. Zhang, Y. Tian, N. Shabanov and R Myneni

*Geography Department, Boston University, 675 Commonwealth Avenue, Boston, MA 02215*

#### **Summary of the algorithm**

The objective of our effort is to develop a radiative transfer based synergistic algorithm for estimation of global leaf area index (LAI) and fraction of photosynthetically active radiation absorbed by vegetation (FPAR). The algorithm consists of a main procedure that exploits the spectral information content of MODIS measurements and the angular information content of MISR measurements to derive accurate estimation of LAI and FPAR. Should this main algorithm fail, a back-up algorithm is triggered to estimate LAI and FPAR using vegetation indices. Both algorithms are capable of executing in MODIS-only or MISR-only mode, should cloud contamination, data frequency and spatial or temporal resolution requirements hinder a joint MODIS/MISR mode of operation. The MODIS-only mode of the algorithm requires a land cover classification that is compatible with the radiative transfer model used in their derivation. Such a classification based on vegetation structure was proposed and it is expected to be derived from the MODIS Land Cover Product. Therefore, our algorithm has interfaces with the MODIS/MISR surface reflectance product and the MODIS Land Cover Product.

#### **Summary of work performed**

- A new method to describe non-linear spectral variation of ground reflectance was developed. The Look-up-Table is now finalized for use with the at launch MODIS LAI/FPAR algorithm.
- The MODIS Look-up-Table and algorithm code have been finalized and delivered to the University of Montana.
- Prototyping of the LAI/FPAR algorithm with atmospherically corrected SeaWiFS (Sea-viewing Wide Field-of-view Sensor) and LASUR-AVHRR (LAnd SURface Reflectances derived from the Advanced Very High Resolution Radiometer) data.
- The two papers submitted to the EOS-AM special issue of Journal of Geophysical Research were positively reviewed.
- Two posters displaying the functionality of the algorithm and its results were prepared. They will be presented at the next MODIS Science Team Meeting.

## **Prototyping of the MODIS LAI/FPAR algorithm**

This report contains results on global LAI and FPAR fields estimated with the MODIS LAI/FPAR algorithm from the SeaWiFS (Sea-viewing Wide Field-of-view Sensor) and LASUR-AVHRR (LAnd SURface Reflectances derived from the Advanced Very High Resolution Radiometer) data. The objectives were as follows:

- Analyze global LAI/FPAR fields derived with the MODIS LAI/FPAR algorithm from the SeaWiFS and LASUR data.
- Analyze the situations when the algorithm fails.
- Assess the influence of uncertainties in surface reflectances on the quality of the LAI/FPAR product.
- Analyze the use of various combinations of spectral bands to produce the LAI/FPAR product.

## Updates to the Look-up-Table

When prototyping the LAI/FPAR product it was found that the assumption of a linear variation of ground reflectance with respect to wavelength in our articles [*Knyazikhin et al.*, 1997a, 1997b] and the MISR ATB [*Diner et al.*, 1998] was incorrect. We developed a new method to describe the non-linear nature of spectral ground reflectance. An update to the Look-up-Table containing 25 patterns of spectral ground reflectances evaluated from the soil reflectance model of *Jacquemoud et al.*, [1992], using model inputs presented in *Barret et al.*, [1993] was done. Figure 1 demonstrates 10 patterns of spectral ground reflectances for grasslands (Biome 1).

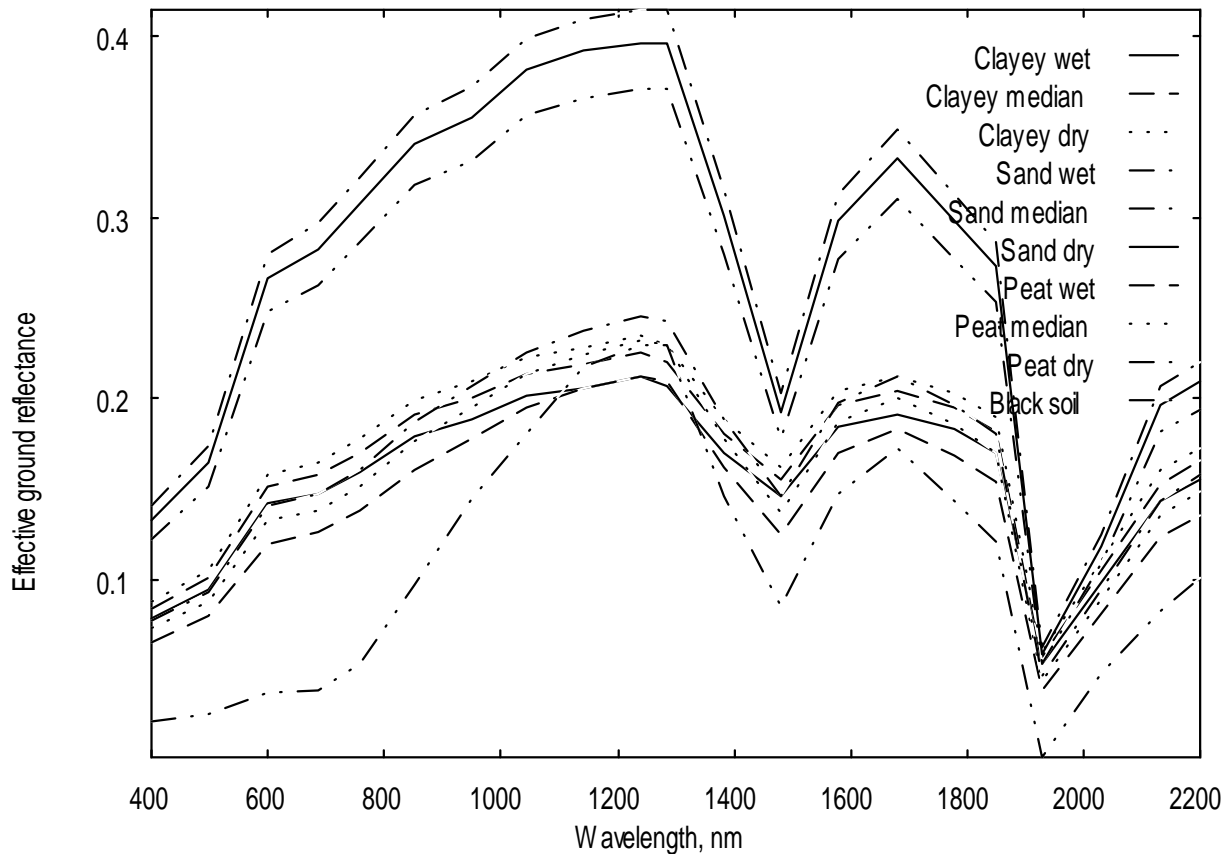


**Figure 1.** Spectral variation of effective ground reflectance

## Data used

SeaWiFS (Sea-viewing Wide Field-of-view Sensor) data set includes global daily atmospherically corrected surface reflectances at 412, 443, 490, 510, 555, 670, 765, 865 nanometers. We used surface reflectances at 443, 555, 670 and 865 nm at 8 kilometer resolution for the period 18 Sep – 12 Oct 1997.

LASUR (LAnd SURface Reflectances) is a data set of atmospherically corrected surface reflectances in the red (572-698 nm) and Near-InfraRed (NIR, 716-985 nm) channels of the Advanced Very High Resolution Radiometer (AVHRR) at global scale (1/7,1, and 5 square degree resolution; one week temporal resolution) for 1989 and 1990.

BCM (Biome Classification Map) containing the distribution of six canopy structural types (biomes). This data set was derived from AVHRR Pathfinder data set [Myneni *et al.*, 1997] and, thus, is independent on the BRF data sets used. Contrary to the SeaWiFS and LASUR data sets, the BCM is the static file, i.e., it is a time-independent data set. This data set was taken as a prototype of the MODIS Land Cover Product which is required by the MODIS LAI/FPAR algorithm (version2.1).

## Uncertainties

Both atmospherically corrected BRF's (Bi-directional Reflectance Factor) and their uncertainties are inputs to the algorithm. However, the SeaWiFS and LASUR data sets have no information on the uncertainties in BRF'S. Therefore, we used the following simple formula to describe this input variable:

$$\sigma(\lambda) = \varepsilon_{\lambda} \cdot r_{\lambda}(\Omega, \Omega_0) \quad (1)$$

Here  $r_{\lambda}(\Omega, \Omega_0)$  is the modeled BRF;  $\Omega$  and  $\Omega_0$  are view and sun directions and  $\varepsilon_{\lambda}$  is the goodness of fit parameter showing relative inaccuracy with respect to the measured BRF. The same formula is used by the MODIS LAI/FPAR algorithm (version 2.1), which was delivered to the University of Montana, our MODIS collaborators. A special technique was developed by the MISR team to evaluate uncertainties in retrieved canopy reflectances [Martonchik *et al.*, 1998]. Therefore, both atmospherically corrected canopy reflectances, BHR's (BiHemispherical Reflectance) and BRF's, and their uncertainties are inputs for our MISR version of the algorithm. In our prototyping activities, the value  $\varepsilon_{\lambda}$  was supposed to be wavelength independent. In the results presented here, its value was 0.2, which was derived by analyzing the retrieved LAI and FPAR values (next sections).

## Execution of the algorithm

We ran the algorithm for each pixel using SeaWiFS, LASUR and BCM data sets. Results presented here are referred to pixels classified by the BCM as biome 1 (Grasses and Cereal Crops) and to July 10-17, 1990 (LASUR) and September 22, 1997 (SeaWiFS). The algorithm was executed for every pixel, whether it was vegetated or not. If the main procedure failed, the back-up algorithm was not executed in this investigation. A detailed description of the back-up algorithm is presented in [Myneni *et al.*, 1997]. The MODIS version was used to retrieve FPAR values.

## Success index

The following characteristics of the *main procedure* are used in this report.

A pixel for which the algorithm retrieved a value of LAI and FPAR is termed as a *successful pixel*.

A pixel for which the algorithm failed is termed as an *unsuccessful pixel*.

The ratio of the number of successful pixels to the total number of pixels is the *success index*.

Figure 2 demonstrates the dependence of the success index on the goodness of fit parameter  $\epsilon$ . The success index increases with the increase of  $\epsilon$ . However the quality of LAI/FPAR product decreases with the increase of the goodness of fit parameter. If  $\epsilon$  is underestimated, the algorithm fails when real uncertainties in surface reflectances are greater than one determined by Eq. (1). If, however, the goodness of fit parameter is overestimated, the algorithm can produce LAI/FPAR values for non-vegetated pixels. Therefore, there should be a critical goodness of fit parameter  $\epsilon^*$  for which Eq. (1) optimally approximates real uncertainties. A solution of the following problem was taken as the critical value: find such  $\epsilon$  for which 95% of unsuccessful pixels are non-vegetated. Solutions to this problem were 0.15 for the LASUR, and 0.20 for the SeaWiFS data.

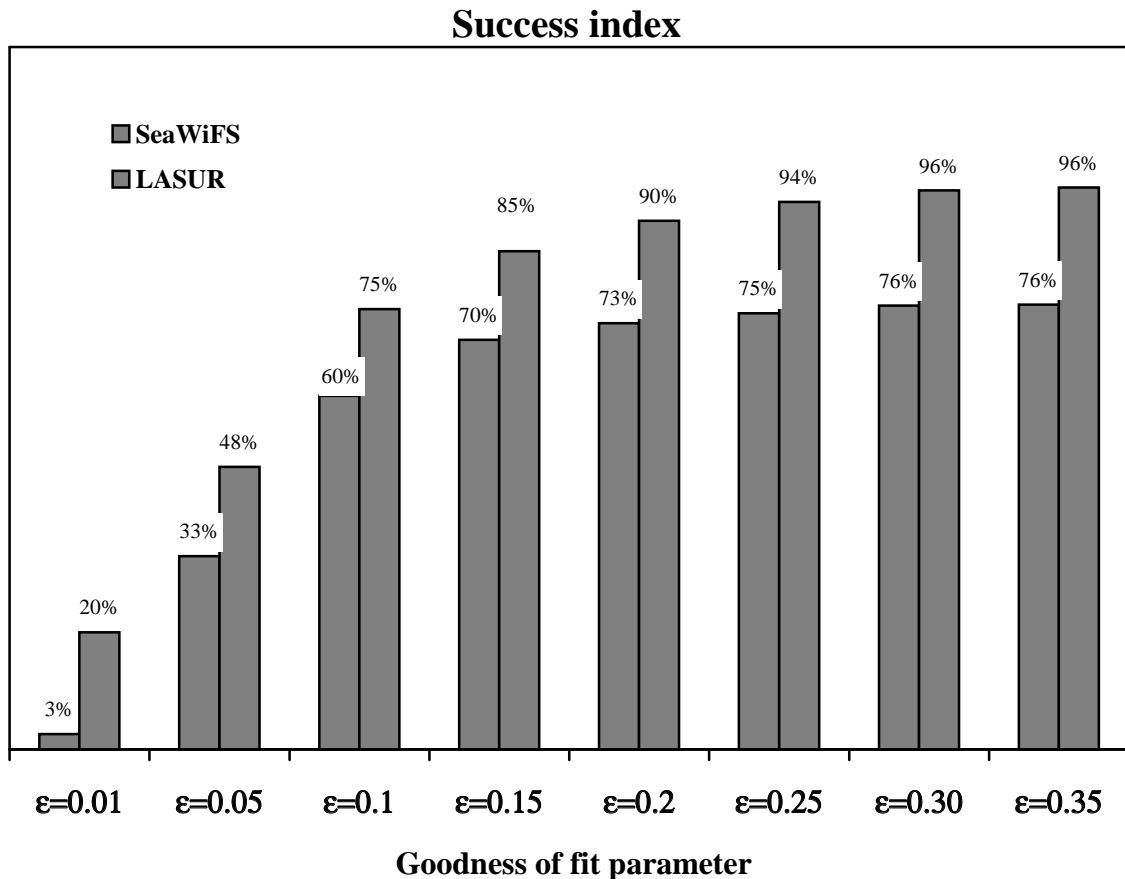


**Figure 2.** Dependence of the success index on the goodness of fit parameter  $\epsilon$ . The optimum values of  $\epsilon$  are 0.20 for the SeaWiFS and 0.15 for LASUR data.

## Test of physics

Figure 3 demonstrates the distributions of retrieved values of LAI and FPAR with respect to the SeaWiFS and LASUR NDVI fields. Two bands, 670 and 865 nm, from the SeaWiFS data set were used to evaluate LAI and FPAR. The LAI-NDVI and FPAR-NDVI relationships derived from the algorithm correspond to those reported in literature.

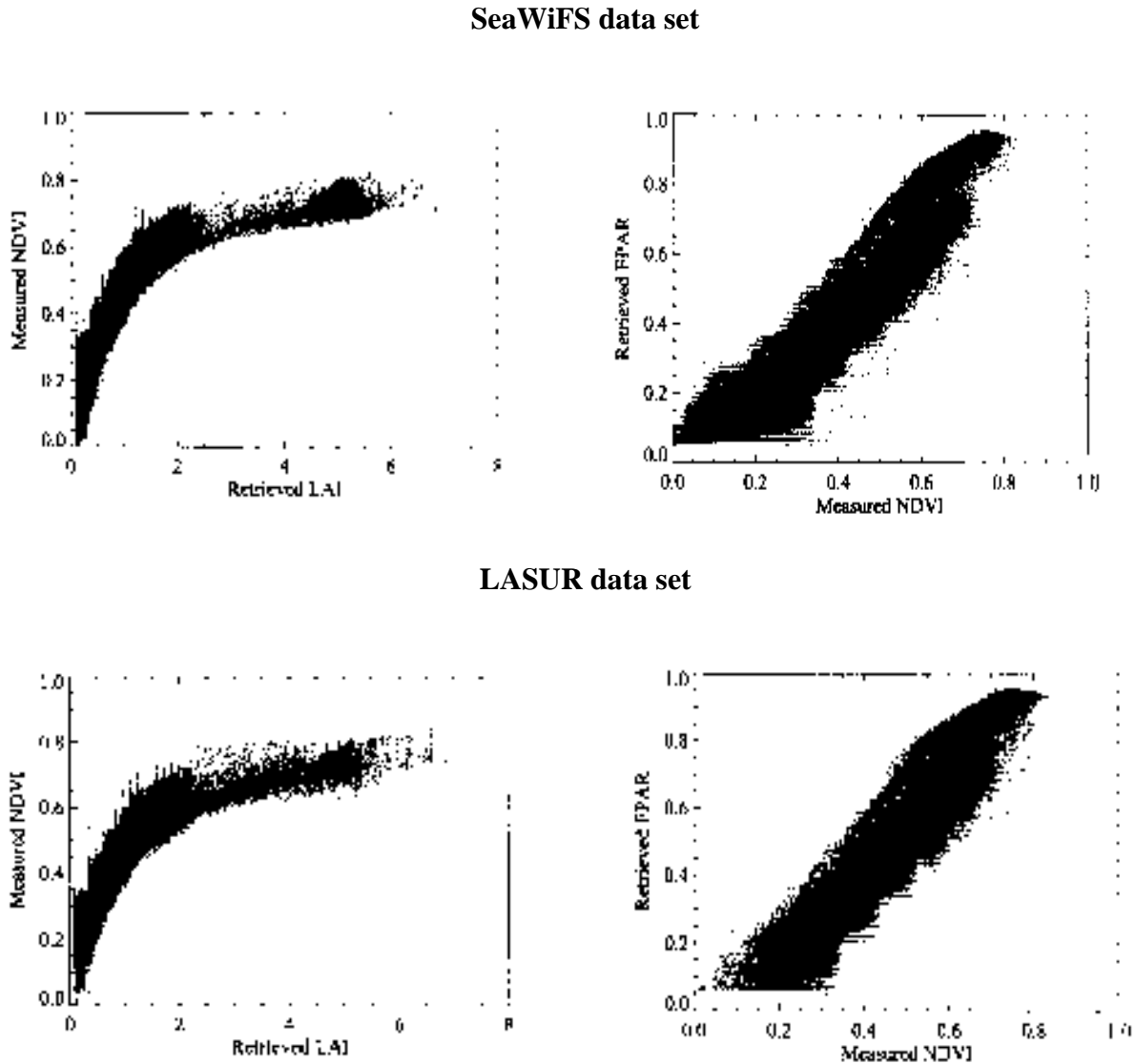
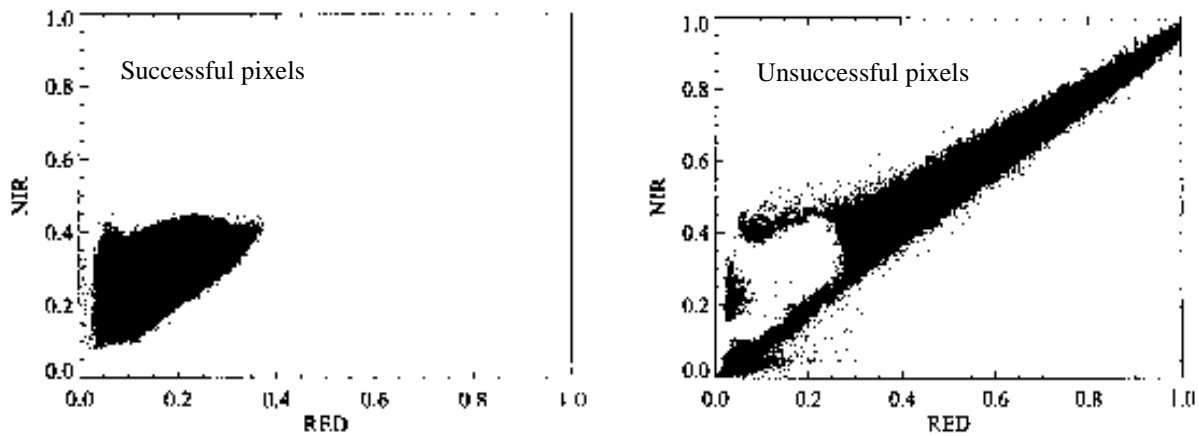


**Figure 3.** LAI-NDVI and NDVI-FPAR relationships derived from the SeaWiFS and LASUR data sets the MODIS LAI/FPAR algorithm. The goodness of fit parameter was 0.20. The success indices were 0.73 for SeaWiFS and 0.9 for LASUR data sets, respectively.

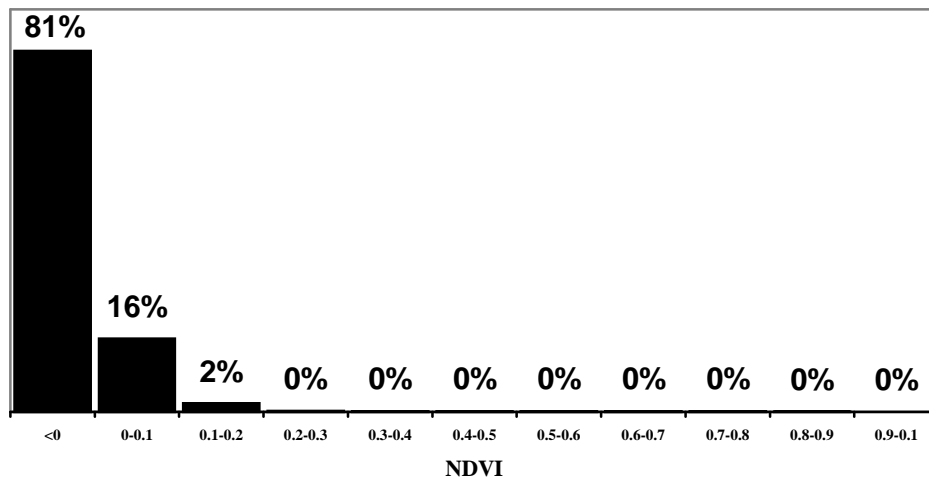
## Distribution of unsuccessful pixels

Figure 4 demonstrates the distribution of pixels from SeaWiFS data set (Grasses and Cereal Crops) with respect to their reflectances at near-infrared and red wavelengths. The left panel shows successful, and the right panel unsuccessful pixels. The success index is 0.73. Figure 5 shows the distribution of unsuccessful pixels with respect to the NDVI values. One can see that 81% of unsuccessful pixels have a negative value of NDVI. The second class of unsuccessful pixels (16%) is one where NDVI values were between 0 and 0.1. Thus, 97% of unsuccessful pixels can not be considered as vegetated pixels.

This example demonstrates that the algorithm mainly fails when the pixels are non-vegetated or data are corrupted due clouds or atmosphere effect provided goodness of fit parameter is chosen correctly.



**Figure 4.** Distribution of pixels with respect to their reflectances at near-infrared and red wavelengths derived from the SeaWiFS data set (September 22, 1997). The left plot shows all pixel for which the algorithm was successful. The right plot shows those pixels for which the algorithm failed. The algorithm was applied to every pixel marked in the BCM data set as Biome 1 (Grasses and Cereal Crops). The number of successful pixels was 73% the goodness of fit was 0.2 in this example.



**Figure 5.** Distribution of "unsuccessful" pixels with respect to NDVI values. One can see that unsuccessful pixels are mainly those for which the NDVI is less than 0.1, that is, non-vegetated pixels.

## Using various combinations of the instrument spectral bands in the retrieval

Figures 6 and 7 demonstrate the LAI-NDVI, NDVI-FPAR relationships, and the distribution of successful and unsuccessful pixels in the NIR-RED plane. These relationships were derived from the SeaWiFS data set using Red (670 nm), Near-infrared (865 nm), Blue (443 nm) spectral bands. Figures 8 and 9 show the same relationships which, however, were obtained by using Red (670 nm), Near-infrared (865 nm), Green (555 nm) spectral bands. If NDVI was less than 0.1, the pixel was considered to be non-vegetated, and the algorithm was not executed. In these examples, therefore, the success index was calculated as the ratio of the number of successful pixels to the total number of pixels for which  $NDVI > 0.1$ .

The use of the blue band results in poor retrievals. The following arguments can be presented. The optical properties of foliage elements at blue and red wavelengths are similar. Thus, the surface reflectances are comparable in magnitude. However, atmospheric effect at blue band is much stronger than at the red band. As a result, the uncertainties in the atmospherically corrected BRF's data are greater at blue than at red band. In prototyping the LAI/FPAR, product we assumed that uncertainties in LASUR and SeAWiFS data sets were wavelength independent. Thus, the algorithm processes the blue and red BRF's with equal weight. The use of blue BRF, therefore, results in poorer retrievals. Holding the goodness of fit parameter  $\epsilon$  constant, all combinations of spectral bands without the blue provide better results than ones including the blue band. Table 1 summarizes the use of different combinations of spectral bands.

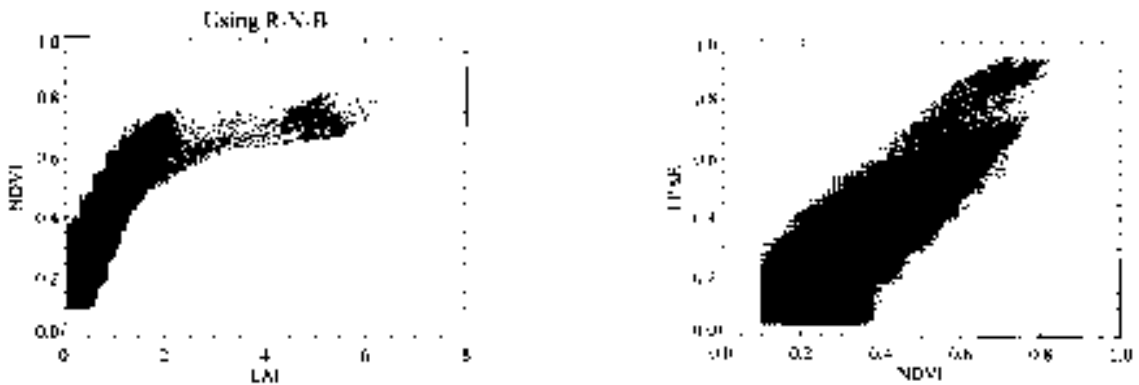


**Figure 6.** NDVI-LAI and FPAR-NDVI relationships derived from the SeaWiFS data sets using Red (670 nm), Near-infrared (865 nm) and Blue (443 nm) spectral bands.

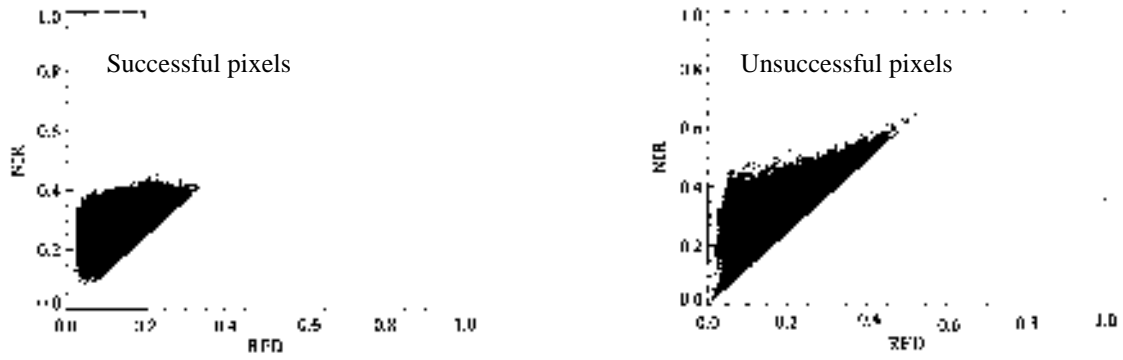


**Figure 7.** Distribution of pixels with respect to their reflectances at near-infrared and red wavelengths derived from the SeaWiFS data set, using Red (670 nm), Near-infrared (865 nm) and Blue (443 nm) spectral bands. The left panel shows all pixels for which the algorithm was successful. The right panel contains those pixels for which the algorithm failed. The goodness of fit parameter  $\epsilon$  was 0.20. The success index is 0.75 estimated as the ratio of the number of successful pixels to the total number of pixels for which NDVI>0.1 in this example.

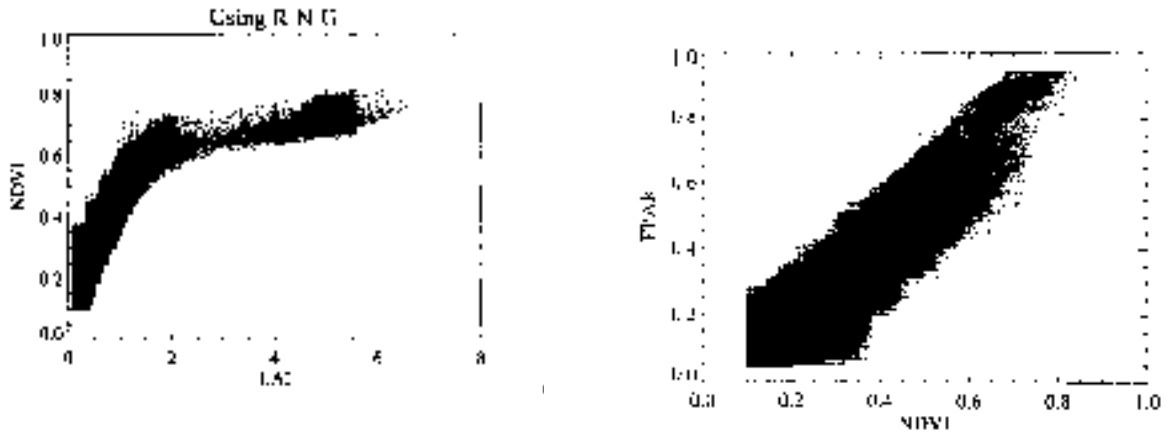


**Figure 8.** NDVI-LAI and FPAR-NDVI relationships derived from the SeaWiFS data sets using Red (670 nm), Near-infrared (865 nm) and Green (555 nm) spectral bands.

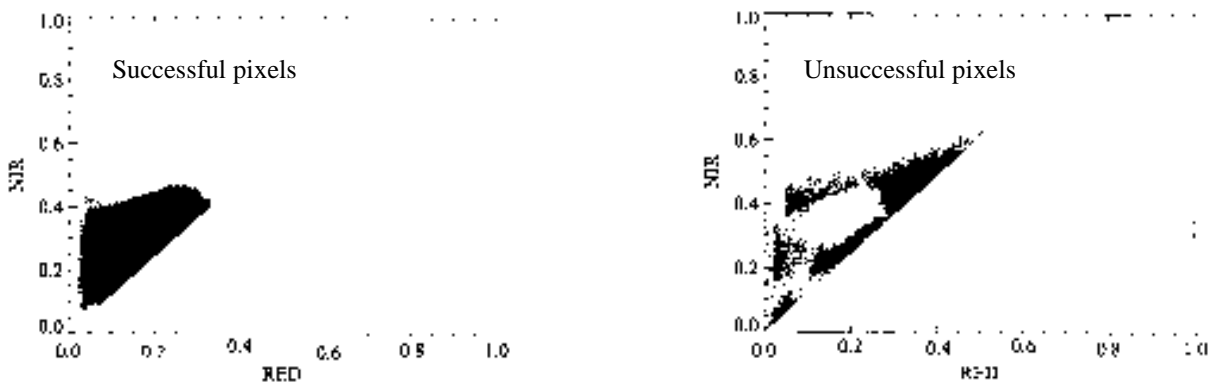


**Figure 9.** Distribution of successful (left) and unsuccessful (right) pixels derived from the SeaWiFS data set, using Red (670 nm), Near-infrared (865 nm) and Green (555 nm) spectral bands. The goodness of fit parameter  $\epsilon$  was 0.20. The success index calculated as in figure 5 is 0.95.

**Table 1.** The success index\* for various combinations of spectral bands used to retrieve LAI and FPAR.

Spectral bands used				Success index, %
NIR	Red	Blue	Green	
x	x			96.8
x	x		x	95.0
	x		x	94.9
x			x	94.8
x		x		86.5
x		x	x	77.8
x	x	x	x	77.8
x	x	x		75.2

\*The success index was calculated here as the ratio of number of successful pixels to the total number of pixels for which NDVI>0.1. Values of the index are expressed in %.

## Prototype of the MODIS LAI/FPAR data standard product

SeaWiFS data. The algorithm was applied to daily surface reflectance data at the 8 km resolution for all days from 18 Sep to 12 Oct 1997. For each pixel, LAI and FPAR values corresponding to the maximum NDVI during this period are shown in Figure 10.

LASUR data. The above algorithm was applied to the weekly surface reflectance data (8 km) for 4 weeks in January and for 4 weeks in July. Figure 11 shows the color-coded images of global LAI in January and in July composited based on maximum NDVI during those four weeks. The global FPAR images in the same months are presented in Figure 12.

## Lessons learned

1. The fundamental physical principle, the law of energy conservation, is the basis of our LAI/FPAR algorithm. A key idea in incorporating this law in the algorithm is the use of the critical eigenvalue to relate canopy structure and optical properties of phytoelements. The critical eigenvalue and the unique positive eigenvector corresponding to this eigenvalue express the law of energy conservation in a compact form. Although the use of such an approach was theoretically justified in our papers [Knyazikhin *et al.*, 1997a, 1997b], no evidence of its functionality was presented. Results from prototyping of the LAI/FPAR product demonstrate not only its ability to produce the global LAI and FPAR fields but also to use all information provided by MODIS instrument.
2. The algorithm mainly fails if a pixel is non-vegetated or data is corrupted due to clouds or atmospheric effect.
3. The algorithm can use all spectral information (bands 1 through 7) of the MODIS instrument. However, the quality of the retrievals can not be better than the quality of the worst spectral BRF, if uncertainties in spectral BRF's are not available. Evaluation of the uncertainties in atmospherically corrected surface reflectances [Martonchick *et al.*, 1998] is critical to improve the quality of the LAI/FPAR product, and to realize the full potential of the MODIS and MISR instruments.
4. If uncertainties in atmospherically corrected surface reflectances are not available, the use of NIR, Red, and Green spectral bands are optimal.

## References

- Baret, F., S. Jacquemoud, and J.F. Hanocq, The soil concept in remote sensing, *Remote Sens. Rev.*, 7, 65-82, 1993.
- Diner, D.J., W.A. Abdou, H.R. Gordon, R.A. Kahn, Yu. Knyazikhin, J.V. Martonchik, S. McMuldroy, R.B. Myneni, R.A. West, Level 2 Ancillary Products and Datasets Algorithm Theoretical Basis, California Institute of Technology, Jet Propulsion Laboratory, JPL internal document D-13402, Rev. A, 1998.
- Jacquemoud, S., F. Barret, and J.F. Hanocq, Modeling spectral and bidirectional soil reflectance, *Remote Sens. Environ.*, 41, 123-132, 1992.
- Knyazikhin, Yu., J.V., Martonchik, R.B. Myneni, D.J. Diner, and S. Running, Synergistic algorithm for estimating vegetation canopy leaf area index and fraction of absorbed photosynthetically active radiation from MODIS and MISR, *J. Geophys. Res.*, 1997a (submitted for publication).
- Knyazikhin, Yu., J.V. Martonchik, D.J. Diner, R.B. Myneni, M.M. Verstraete, B. Pinty, and N. Gobron, Estimation of vegetation canopy leaf area index and fraction of absorbed photosynthetically active radiation from MISR data, *J. Geophys. Res.*, 1997b (submitted for publication).
- Martonchik, J.V., D.J. Diner, B. Pinty, M.M. Verstraete, R.B. Myneni, Y. Knyazikhin, and H.R. Gordon, Determination of land and ocean reflective, radiative and biophysical properties using multi-angle imaging, *IEEE Trans. Geosci. Remote Sens.*, 1997 (accepted for publication).
- Myneni, R.B., R.R. Nemani, and S.W. Running, Estimation of global leaf area index and absorbed PAR using radiative transfer model, *IEEE Trans. Geosci. Remote Sens.*, 35, 1380-1393, 1997.